AMERICAN ACADEMY OF OPHTHALMOLOGY®

Progression Dynamics of Early versus Later Stage Atrophic Lesions in Nonneovascular Age-Related Macular Degeneration Using Quantitative OCT Biomarker Segmentation

Leonard M. Coulibaly, MD,[1] Gregor S. Reiter, MD, PhD,[2] Philipp Fuchs, MD,[1] Dmitrii Lachinov, MSc,[2] Oliver Leingang, PhD,[2] Wolf-Dieter Vogl, Dipl-Ing, PhD,[3] Hrvoje Bogunovic, PhD,[2] Ursula Schmidt-Erfurth, MD[1,2]

Purpose: To investigate the progression of geographic atrophy secondary to nonneovascular age-related macular degeneration in early and later stage lesions using artificial intelligence–based precision tools.

Design: Retrospective analysis of an observational cohort study.

Subjects: Seventy-four eyes of 49 patients with $\geq$ 1 complete retinal pigment epithelial and outer retinal atrophy (cRORA) lesion secondary to age-related macular degeneration were included. Patients were divided between recently developed cRORA and lesions with advanced disease status.

Methods: Patients were prospectively imaged by spectral-domain OCT volume scans. The study period encompassed 18 months with scheduled visits every 6 months. Growth rates of recent cRORA-converted lesions were compared with lesions in an advanced disease status using mixed effect models.

Main Outcome Measures: The progression of retinal pigment epithelial loss (RPEL) was considered the primary end point. Secondary end points consisted of external limiting membrane disruption and ellipsoid zone loss. These pathognomonic imaging biomarkers were quantified using validated deep-learning algorithms. Further, the ellipsoid zone/RPEL ratio was analyzed in both study cohorts.

Results: Mean (95% confidence interval [CI]) square root progression of recently converted lesions was 79.68 (95% CI, −77.14 to 236.49), 68.22 (95% CI, −101.21 to 237.65), and 84.825 (95% CI, −124.82 to 294.47) mm/half year for RPEL, external limiting membrane loss, and ellipsoid zone loss respectively. Mean square root progression of advanced lesions was 131.74 (95% CI, −22.57 to 286.05), 129.96 (95% CI, −36.67 to 296.59), and 116.84 (95% CI, −90.56 to 324.3) mm/half year for RPEL, external limiting membrane loss, and ellipsoid zone loss, respectively. RPEL ($P = 0.038$) and external limiting membrane disruption ($P = 0.026$) progression showed significant differences between the 2 study cohorts. Further recent converters had significantly ($P < 0.001$) higher ellipsoid zone/RPEL ratios at all time points compared with patients in an advanced disease status (1.71 95% CI, 1.12–2.28 vs. 1.14; 95% CI, 0.56–1.71).

Conclusion: Early cRORA lesions have slower growth rates in comparison to atrophic lesions in advanced disease stages. Differences in growth dynamics may play a crucial role in understanding the pathophysiology of nonneovascular age-related macular degeneration and for the interpretation of clinical trials in geographic atrophy. Individual disease monitoring using artificial intelligence–based quantification paves the way toward optimized geographic atrophy management.

Financial Disclosure(s): The author(s) have no proprietary or commercial interest in any materials discussed in this article. *Ophthalmology Retina 2023;7:762-770*

Geographic atrophy (GA) is considered the late-stage manifestation of nonneovascular age-related macular degeneration (AMD). More than 5 million people globally are affected by severe loss of visual function caused by GA, and estimations predict an exponential increase because of the aging population worldwide.[1] GA secondary to nonneovascular AMD can be considered a major burden for affected patients' quality of life and is a contributor to irreversible retinal blindness worldwide.[1,2]

Atrophic lesions in AMD often evolve through different stages but are always characterized by well-demarked areas in the macular region with loss of retinal pigment epithelial (RPE) and/or overlaying photoreceptor degeneration.[3] The classification of atrophy meetings (CAM) program proposed OCT as reference standard in the diagnosis and staging of these atrophic lesions. Complete RPE and outer retinal atrophy (cRORA) succeeds incomplete RPE and outer retinal atrophy (iRORA) and defines the end stage in

https://doi.org/10.1016/j.oret.2023.05.004
ISSN 2468-6530/23

the evolution of atrophic lesions. To differentiate between iRORA and cRORA, atrophic lesions must fulfill a triumvirate of characteristics on OCT imaging: RPE loss (RPEL) and choroidal hypertransmission over 250 μm accompanied by signs of overlaying photoreceptor degeneration. Outer nuclear layer thinning, external limiting membrane loss (ELML), and ellipsoid zone (EZ) or interdigitation zone loss was qualified as signs for photoreceptor degeneration.[4]

During the natural history of GA progression, cRORA lesions continuously grow, advancing the decline of affected patients' visual acuity (VA). This progression might be considered slow as it develops over the time span of years; nonetheless, available therapeutic options halting or slowing the disease progression are limited.[5] Meanwhile, a certain level of interindividual and intraindividual variability in progression speed has been observed,[6] showcasing lesion growth rates ranging from 0.27 to 0.40 mm/year.[7] The causes for these discrepancies have been the object of numerous publications over the last years. Some studies laid emphasis on lesion focality and configuration, as lesion multifocality correlates with higher GA enlargement rates.[8] Other studies highlighted a topographic impact, suggesting that lesions involving the macular center point have a slower growth rate compared with nonfoveal lesions.[9] Further specific biomarkers such as hyperreflective foci or subretinal drusenoid deposits (SDDs) have been identified as having a significant correlation with faster disease progression.[10] Another potential hypothesis on divergent cRORA lesion growth rates suggests that specific time points in the natural progression of the disease are linked to a more or less rapid lesion growth.[9,11]

The development of cRORA and risk factors promoting rapid disease progression are not fully understood. Data on the early stages of the disease are rare, because of its subclinical development with preserved VA. We therefore propose an artificial intelligence (AI)-supported OCT biomarker quantification to assess GA lesion growth rates. Our study's aim is to compare growth rates of recently developed cRORA lesions with more advanced stages of the disease. In the light of recent advances concerning the approval of therapeutic agents with the potential to reduce disease progression,[12] a deeper understanding of the early natural course of GA will be crucial. This study's results will be important for the identification of the optimal time point for the first intervention. Further, they will help in the interpretation of ongoing trials as well as in the setup of future trials as we might be able to identify a bias because of the time point of inclusion during the natural disease progression.

Methods

This study adhered to the tenets of the Declaration of Helsinki and was approved by the Ethics Committee of the Medical University of Vienna. Patients with cRORA secondary to nonneovascular AMD were only included in the study after providing written informed consent. Atrophic lesions were classified as cRORA in accordance with the consensus definition proposed by the CAM group in 2018.[4] In the event both eyes were eligible, both were included in the study and considered in the statistical model. Patients showing signs of active macular neovascularization or having a history of anti-VEGF therapy were excluded from the study. Additionally, a merging between the cRORA lesion and a peripapillary atrophy was considered an exclusion criterium as the exact cRORA borders and subsequently the area of lesion growth could not be determined reliably.

Patients were divided into 2 study cohorts. Cohort 1 was considered the "recent cRORA" study arm and had a documented conversion from iRORA to cRORA during the 6 months before study inclusion. Documented conversion means that an OCT scan without cRORA was available in the 6 months before conversion. Cohort 2 was composed of patients with a documented presence of cRORA for $\geq$ 2 years preceding inclusion in the study and was therefore considered the "later stage or advanced cRORA" study arm. The identification of the conversion time point from iRORA to cRORA was performed by a retinal expert on OCT volume scans before inclusion in the study.

Scheduled visits were held every 6 months over a period of 18 months. A 6 × 6-mm volume scan, corresponding to a pixel area of approximately 120 × 11.25 μm^2, covering the central 20° was performed with a spectral-domain (SD)-OCT (Spectralis HRA+OCT; Heidelberg Engineering) device during every visit. The number of B-line scans per volume during the baseline visit varied between 49 and 97 B-scans but was kept consistent regarding the follow-up visits.

Image Analysis (Biomarker Segmentation)

The pathognomonic biomarkers for cRORA of RPEL, ELML and ellipsoid zone loss (EZL) were quantified for every visit within the central 6 mm of the macula. Additionally, baseline scans were graded by a retinal expert for the presence of SDDs, lesion locality, and lobularity. Lesion locality was graded according to presence or absence of foveal sparing. Lesion lobularity was assessed through 3 categories: unifocal (a single lobule), multifocal (multiple singular lobules), or multilobular (coalescence of multiple lobules to a single atrophy patch). All measured biomarkers are summarized under Table 1. The AI algorithms employed in this study are based on validated deep-learning models designed for GA segmentation. All 3 segmentation algorithms use fully convolutional neural networks with projective skip connections to compress and project encoded 3-dimensional OCT features into 2-dimensional output space.[13] The convolutional neural networks use an innovative enhanced U-shaped structure enabling a pixel-accurate segmentation of the target structures. They were trained on an in-house (Vienna Clinical Trial Center at the Department of Ophthalmology and Optometry, Medical University of Vienna) dataset and evaluated on an extensive set of reference manual annotations of the FILLY trial (ClinicalTrials.gov Identifier: NCT02503332). The algorithm's performance was previously published, and accuracy of the biomarker segmentations can be considered high.[13–15] All automated segmentations were verified and, if necessary, manually corrected by an expert grader.

Study End Points

The primary end point consisted of the half yearly growth rates of RPEL. Applying the definition proposed by the CAM classification, the disruption of the RPE must be considered as the limiting factor while estimating cRORA lesion size. Half yearly growth rates of ELML and EZL were considered secondary end points. The growth rate of each biomarker was the difference between the measurements obtained during half yearly scheduled visits. The growth rate was calculated after applying a square root transformation. The results will therefore be assessed in mm/half year.

Figure 1 showcases the performance of the automated segmentation tool for a patient with an advanced disease stage.

Additional secondary end points included putative effects of the various biomarkers visible during the baseline visit (see Table 2) on our primary outcome. These baseline features included sex, number of B-scans, presence of SDDs, lesion lobularity, and locality. Another secondary outcome was a comparison of the ratio between EZL and RPEL between the 2 study cohorts.

Statistical Analysis

Linear mixed models (LMMs) were calculated to investigate the impacts on the growth of atrophy-related biomarkers over a period of 18 months. The areas of RPEL, ELML, and EZL were square root transformed, and the difference between 2 consecutive 6-month visits was used as the dependent variable for each LMM, respectively. Study arm, time point, presence of SDDs, multifocality/-lobularity, presence of foveal sparing, sex, numbers of B-scans, and the interaction between study arm and time point (study arm × time point) were included as fixed factors. A random factor for the eye was specified, which was nested in the random factor for the patient. This allows correction for multiple visits and/or eyes from the same patient. To investigate the difference of pneumatic retinopexy to RPE ratio between freshly converted and previously existing GA eyes, another LMM was calculated with EZL/RPEL ratio as the dependent variable. Study arm, time point, presence of SDDs, multifocality/-lobularity, presence of foveal sparing, sex, numbers of B-scans, and the interaction between study arm and time point (study arm × time point) were included as fixed factors. Model performance was evaluated using the Akaike information criterion, and best model fit was investigated by omitting the least significant factor until no further improvement in Akaike information criterion was achieved. Post hoc pairwise testing for each LMM was performed using Bonferroni correction for multiple testing. Alpha was set to 0.05, thus making a P value < 0.05 significant.

Results

Thirty-four eyes from 26 patients were defined as recent cRORA and included in Cohort 1, whereas 40 eyes from 23 patients fulfilled the criteria for advanced cRORA and were included in Cohort 2. Descriptive statistics of the chosen biomarkers are summarized in Table 2. A chi-square test could not find a significant difference between eyes with the presence of SDDs (X^2 (1, N = 74) = 0.04, $P = 0.842$) or foveal sparing (X^2 (1, N = 74) = 2.273, $P = 0.131$) between the 2 groups.

For the LMM investigating each parameter's (RPEL, ELML, EZL) growth speed, study arm, time point, presence of SDDs, multifocality/-lobularity, presence of foveal sparing, sex, numbers of B-scans, and the interaction between study arm and time point (study arm × time point) were included in the LMM. Ultimately, the factor "number of B-scans" did not contribute to enhancing the performance of each LMM and was therefore omitted from the final models.

Figure 2 showcases the performance of the automated segmentation tool as well as the progression during the study.

Mean overall RPEL was 105.706 µm/6 months (95% CI, −47.905 to 259.318). For the LMM investigating RPE loss, study arm ($P = 0.038$) and the presence of foveal sparing ($P = 0.044$) were the only significant parameters. All other parameters did not reach significance. Growth of RPEL in eyes that recently converted to GA was significantly slower than in eyes that had preexisting GA 79.676 (95% CI, −77.140 to 236.493) vs. 131.737 (95% CI, −22.574 to 286.047) µm/6 months, respectively (see Fig 3A). Growth of RPEL was significantly faster when foveal sparing was present (129.467 [95% CI, −27.009 to 285.944] vs. 81.167 [95% CI, −72.246 to 236.137]) µm/6 months, respectively). The interaction of study arm × time point was not significant but improved overall model performance.

Mean overall ELML was 99.091 (95% CI, −66.735 to 264.918) µm/6 months. For the LMM investigating ELML, study arm ($P = 0.026$) and the presence of foveal sparing ($P = 0.042$) were the only significant parameters. All other parameters did not reach significance. Growth of ELML in eyes that recently converted to GA was significantly ($P = 0.026$) slower than in eyes that had preexisting GA, 68.219 (95% CI, −101.210 to 237.648) versus 129.964 (95% CI, −36.666 to 296.594) µm/6 months, respectively (see Fig 3B). Growth of ELML was significantly faster when foveal sparing was present, 125.606 (95% CI,−43.466 to 294.679) versus 72.577 (95% CI, −93.898 to 239.051) µm/6 months, respectively). The interaction of study arm × time point was not significant but improved overall model performance.

Table 1. Chosen Imaging Biomarkers

Biomarker	Definition	Grading	Time Point
RPE loss (RPEL)	A complete loss or attenuation of the RPE in the central 6 mm	Automatic AI algorithm segmentation and manual correction by retinal expert	Every visit
ELM loss (ELML)	A complete disruption of the ELM in the central 6 mm	Automatic AI algorithm segmentation and manual correction by retinal expert	Every visit
EZ loss (EZL)	A complete loss of the EZ with a tolerance threshold of up to 4 µm (corresponding to 1 pixel on SD-OCT B-line scan)	Automatic AI algorithm segmentation and manual correction by a retinal expert	Every visit
SDDs	Presence of ≥ 5 SDDs in the central 6 mm	Manual grading by retinal expert	At baseline
Lesion locality	Presence of a foveal sparing in the central mm	Manual grading by retinal expert	At baseline
Lesion lobularity	Consideration as unifocal (a single lobule), multifocal (multiple singular lobules), or multilobular (coalescence of multiple lobules to a single atrophy patch)	Manual grading by retinal expert	At baseline

AI = artificial intelligence; ELM = external limiting membrane; EZ = ellipsoid zone; RPE = retinal pigment epithelium; SD = spectral domain; SDD = subretinal drusenoid deposits.

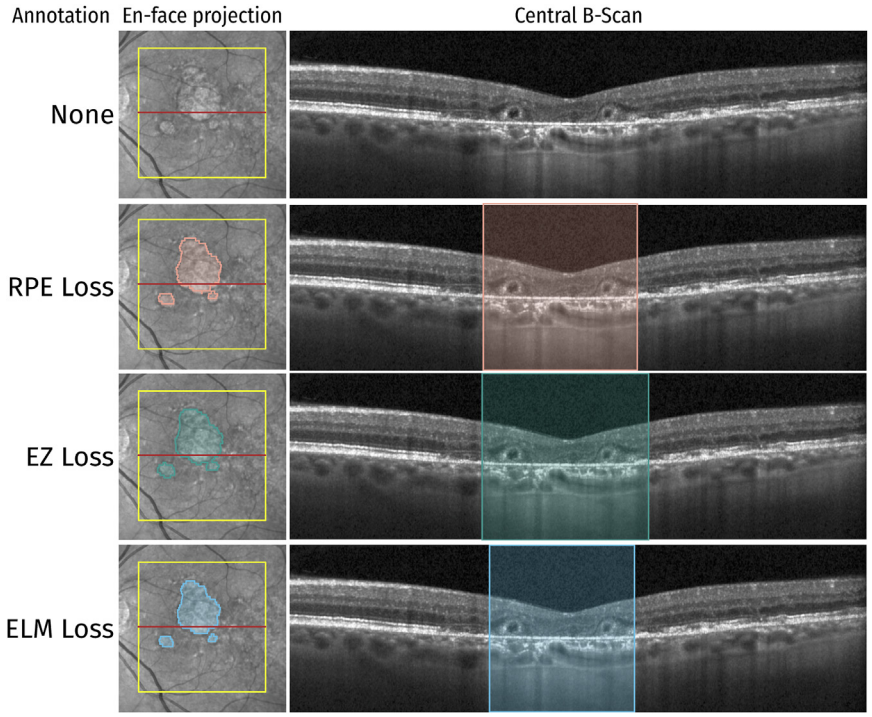

Figure 1. Biomarker segmentation of an advanced complete retinal pigment epithelial and outer retinal atrophy (cRORA) lesion at baseline. Segmentations of cRORA-specific biomarkers (retinal pigment epithelium [RPE] loss [red], ellipsoid zone [EZ] loss [green], and external limiting membrane [ELM] disruption [blue]) on advanced cRORA lesion (conversion > 2 years before baseline visit) at baseline visit.

Table 2. Descriptive Statistics

	Cohort 1: Recent cRORA	Cohort 2: Advanced cRORA	Total
Number of subjects	26	23	49
Number of study eyes	34	40	74
Male/Female	5/29	13/27	18/56
Mean age, yrs	76.1	74.5	75.2
Percentage of eyes with foveal sparing	47% (16)	30% (12)	37.8% (28)
Percentage of eyes with SDDs	20.6% (7)	22.5% (9)	21.6% (16)
Percentage of eyes with unifocal lesions	44.1% (15)	15% (6)	28.4 %
Percentage of eyes with unifocal/multilobular lesions	2.9% (1)	25% (10)	14.9 %
Percentage of eyes with multifocal lesions	52.9% (18)	60% (24)	56.7%
Mean baseline RPE loss in mm^2 ± SD	0.75 ± 0.59	9.79 ± 6.03	6.84 ± 6.85
Mean baseline EZ loss in mm^2 ± SD	2.25 ± 1.89	11.88 ± 7.25	9.06 ± 8.00
Mean baseline ELM loss in mm^2 ± SD	0.67 ± 0.58	8.94 ± 5.91	6.59 ± 6.69
Mean RPEL in µm/half yr (95% CI)	79.68 (−77.14 to 236.49)	131.74 (−22.57 to 286.05)	105.71 (−47.91 to 259.32)
Mean RPEL in mm/yr (95% CI)	0.16 (−0.15 to 0.47)	0.26 (−0.04 to 0.57)	0.21 (−0.96 to 0.52)
Mean ELML in µm/half yr (95% CI)	68.22 (−101.21 to 237.65)	129.96 (−36.67 to 296.59)	99.09 (−66.73 to 264.92)
Mean ELML in mm/yr (95% CI)	0.14 (−0.202 to 0.475)	0.26 (−0.07 to 0.59)	0.12 (−0.13 to 0.53)
Mean EZL in µm/half yr (95% CI)	84.82 (−124.82 to 294.47)	116.84 (−90.56 to 324.3)	100.85 (−106.17 to 307.87)
Mean EZL in mm/yr (95% CI)	0.17 (−0.25 to 0.59)	0.24 (−0.18 to 0.65)	0.2 (−0.21 to 0.62)
Mean EZL/RPEL ratio	1.71 (1.12−2.28)	1.14 (0.56−1.71)	1.42 (0.85−1.99)

cRORA = complete RPE and outer retinal atrophy; CI = confidence interval; ELM = external limiting membrane; ELML = external limiting membrane loss; EZ = ellipsoid zone; EZL = ellipsoid zone loss; RPE = retinal pigment epithelium; RPEL = retinal pigment epithelium loss; SD = standard deviation; SDD = subretinal drusenoid deposit.

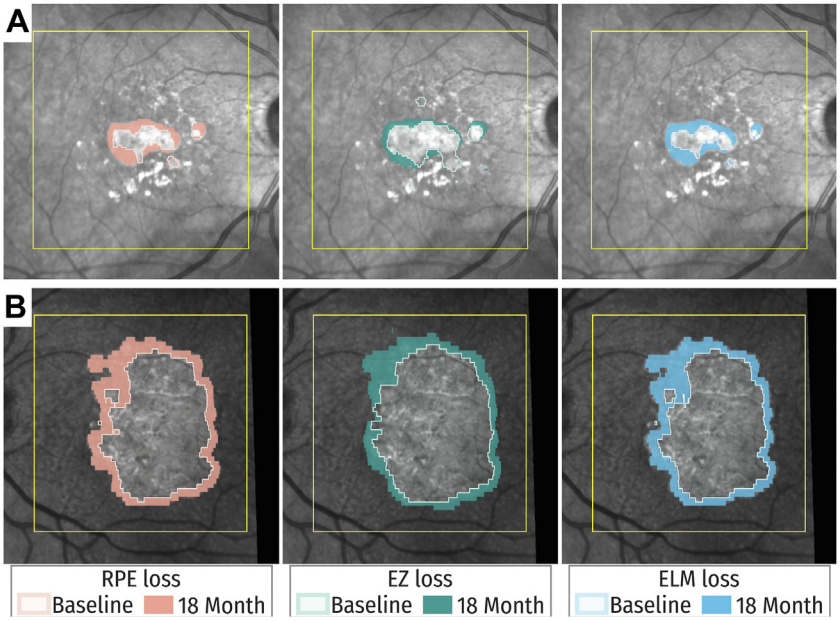

Figure 2. Biomarker segmentation of a recent and advanced complete retinal pigment epithelial and outer retinal atrophy (cRORA) lesion at baseline and 18 months later. En face segmentations of cRORA-specific biomarkers and their respective progression during the study period (retinal pigment epithelium [RPE] loss [red], ellipsoid zone [EZ] loss [green], and external limiting membrane [ELM] loss [blue]). **A,** Patient with a recent conversion to cRORA (within the last 6 months before baseline visit); **B,** Patient with an advanced disease status (documented cRORA for at least the last 2 years).

Compared with RPEL and ELML, study arm and the presence of foveal sparing did not reach significance in the EZL model. Although no significant association between EZL and other factors could be found, descriptive similarities to RPEL and ELML were observed (see Fig 3C). EZL showed higher variances than the other 2 biomarkers, which might be the reason for not reaching the significance level.

The final LMM for EZL/RPEL ratio included the random factors for the eye nested in the random factor in the patient and study visit, study arm, presence of SDDs, multifocality/-lobularity, and presence of foveal sparing as fixed factors. All other parameters, including the interaction of study visit × study arm were omitted to improve model performance and decrease the degrees of freedom of the LMM. Study visit ($P = 0.015$), study arm ($P < 0.001$), and multifocality/-lobularity ($P = 0.035$) were found to have a significant association with EZL/RPEL ratio. Presence of foveal sparing did not reach significance ($P = 0.091$) in our analysis. Fresh converter had significantly higher EZL/RPEL ratios at all-time points (1.716; 95% CI, 1.135−2.296 vs. 1.153; 95% CI, 0.576−1.729, respectively). However, EZL/RPEL ratios appeared to decrease over time but increased with lobularity status (unifocal unilobular < unifocal multilobular < multifocal multilobular). However, a significant pairwise difference was only found in the extreme opposites (unifocal unilobular − multifocal multilobular) after Bonferroni correction ($P = 0.029$).

Discussion

The progression dynamic of GA secondary to non-neovascular AMD has gathered a lot of interest in the last years. This interest is warranted, considering the advances in the development of therapeutics with the potential of slowing disease progression. Major Phase II and III studies examining these new drugs' efficacy and safety have adopted mean GA area growth as their primary end point.[16−18] Identification of biomarkers having an influence on growth rates will be crucial for a comprehensive and in-depth analysis of these studies' results. A topographic assessment of GA lesions, as performed in our study, is necessary to demonstrate interpatient disease progression heterogeneity.[14]

Morphologic disease progression and atrophic lesion growth are conventionally assessed using fundus autofluorescence (FAF), color fundus photography (CFP), en face SD-OCT scans, or macular SD-OCT cube scans.[6,19] An advantage of FAF, CFP, and en face SD-OCT scan is that the imaging process and subsequent GA lesion segmentation is comparably expeditious. Meanwhile, the important amount of data generated during an SD-OCT cube scan leads to an arduous and time-consuming segmentation process, especially if multiple biomarkers are examined. Nonetheless, SD-OCT volume scans are the preferred imaging modality to measure cRORA lesion extension as defined by the CAM classification.[4,20] The cross-sectional images of retinal layers attained through SD-OCT volume scans offer precise insight into the pathologic processes for each involved cell layer.[21] With the introduction of AI algorithms to aid in accurate identification of OCT biomarkers in an automated manner, the time strain caused by the segmentation tasks can be minimized while obtaining excellent visualization and quantification of disease activity. Further, the use of AI algorithms increases segmentation reliability, mitigating intergrader discrepancies in a spectrum of subclinical markers.[22]

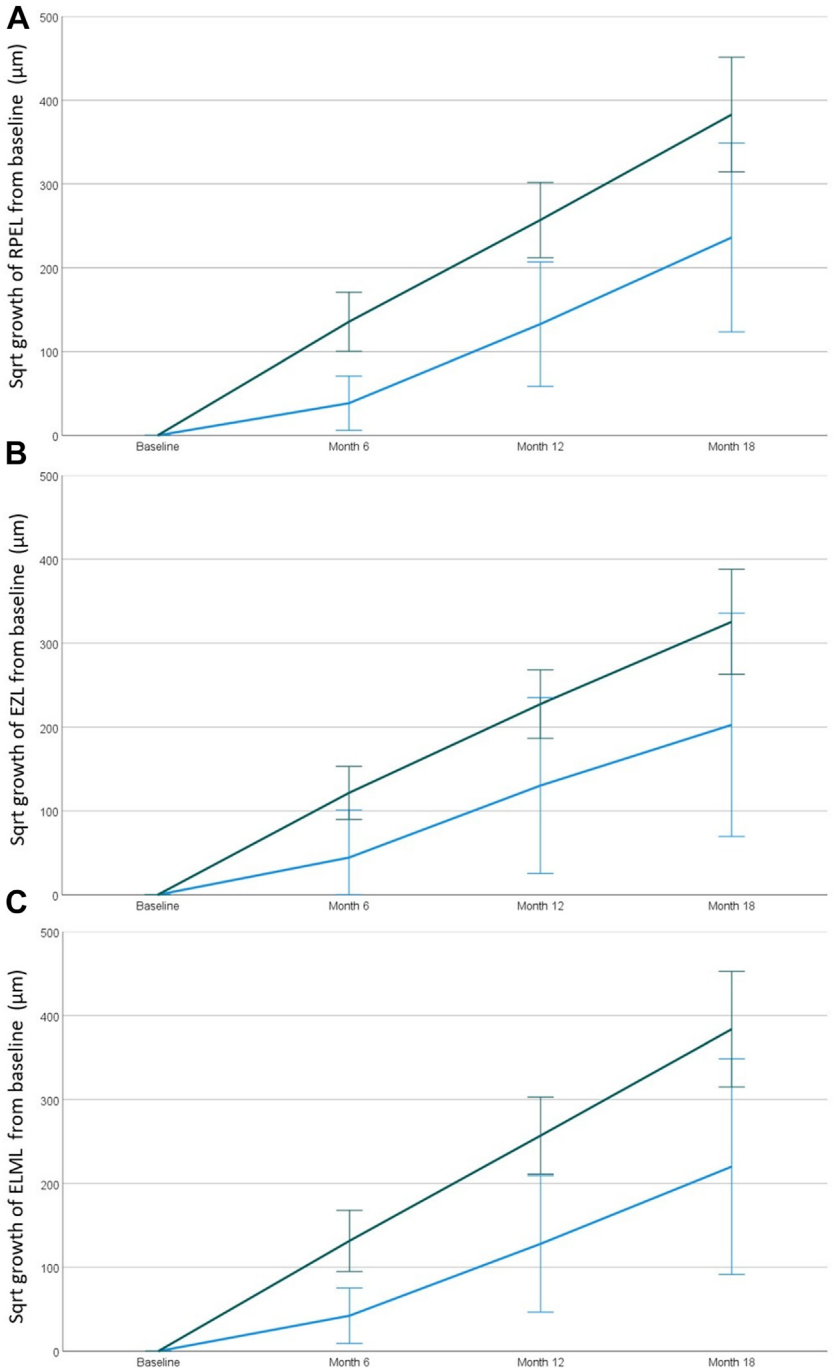

Figure 3. Square root growth rates of complete retinal pigment epithelial and outer retinal atrophy (cRORA) biomarkers. Square root progression from baseline to month 18 for retinal pigment epithelial loss (RPEL) (**A**), ellipsoid zone loss (EZL) (**B**), and external limiting membrane loss (ELML) (**C**) for advanced (green) and recent (blue) cRORA lesions in µm.

To our knowledge, this is the first study that compares growth rates between recently developed and advanced cRORA lesions using disease-specific biomarkers on SD-OCT volume scans with the support of innovative AI-based algorithms.

Presuming a linear progression of a circular lesion with increasing radius, the baseline area of atrophic lesion will be linked to a larger growth rate in mm^2/year in comparison to a smaller lesion. To avoid this bias, numerous publications have showed the benefits of applying a square root transformation.[7,23,24] As we expected large differences in absolute baseline cRORA lesion size between the 2 study cohorts, we considered a square root transformation of the measurements before the calculation of growth rates to be crucial.

The biomarkers labeled RPEL and ELML showed a significantly smaller growth rate in eyes with recently developed cRORA lesions in comparison to patients with advanced cRORA lesions.

A reduced growth rate in the earlier stages of cRORA propagation has been hypothesized by other research groups in recent publications. In a post hoc analysis of CFP from the AREDS2 data set by Keenan et al,[11] slower growth rates at the beginning and at the end of the GA lesion life cycle could be observed. The authors attributed these reduced growth rates to an incomplete establishment of the pathological mechanisms furthering the lesion propagation. A similar hypothesis was presented by Arslan et al[25] while performing an analysis of uncertainty of GA lesion growth. The authors suggested the possibility that GA lesion growth might follow a sigmoidal function rather than a strict linear growth. The presumed toe and shoulder end would present slower growth rates. The toe end of this hypothetical sigmoidal function is represented by the early stages after conversion to cRORA. These patients would often be underrepresented in clinical trials observing GA lesion growth rates due to the subclinical manifestation of small GA lesions. However, these data were based on conventional CFP without comprehensive insight into the realistic morphological composition of GA lesions.

High-resolution OCT-based results from the RPEL, EZL, and ELML growth rates in the advanced study cohort are comparable, although on the lower end of the mean GA growth rate reported by Wang and Ying[7] (0.27−0.40 mm/year) or Keenan et al[11] (0.27−0.30 mm/year). The specific cRORA measurement on SD-OCT, as performed in our study, could lead to smaller growth rates compared with more general GA lesion measurements with other imaging modalities (e.g., CFP or FAF), as performed among others in the above-mentioned reviews. This effect can be attributed to RPE dysmorphia on the GA lesion edges that do not fulfill the CAM criteria for cRORA but might be identified as part of the lesion on FAF imaging.[19,26] Smaller growth rates for very large cRORA lesions at baseline have been previously described.[27] As we did not have any restriction regarding maximal baseline lesion size during our recruitment, some of the patients in the advanced cRORA study cohort might show slower growth rates because of their large baseline size.

The biomarker EZL showed no significant difference between the 2 study arms although descriptive similarities with the other 2 biomarkers were observed (see Fig 3C). One possible reason behind this might be explained by the high variance observed in the entire cohort. The segmentation of EZ reflectivity and its disruption can be challenging.[28] More data will be needed to accurately interpret the growth rate of EZL. In-depth insights into the dynamics of photoreceptor loss in GA warrant attention as recent publications have shown the significant impact of complement inhibitors in slowing photoreceptor decline in GA.[15] Advances in imaging technology might allow a more precise interpretation of the EZ and therefore photoreceptor functionality.

In both our study cohorts the EZL was consistently larger than the RPEL. This is in line with recent observations in the literature describing an outreaching of EZL beyond the borders of the cRORA lesion.[20] EZ and photoreceptor loss has previously been described as a precursor of future RPE atrophy in GA.[20,29−31] Subjects in the fresh converter cohort showed significantly higher EZL/RPEL ratios at all time points than their counterparts in the advanced study cohort. We hypothesize that early cRORA lesions, where the pathologic disease-promoting mechanisms are not established completely, already show early signs of disease activity such as a photoreceptor decline. During the natural course of the disease progression, the ratio between RPEL and EZL decreases due to advancing and secondary "catching-up" of the subsequent RPE degeneration. Nonetheless, we need to consider that EZL/RPEL ratios of recently converted cRORA lesions might still be skewed due to the small lesion size, leading to a higher ratio variability in comparison to more advanced and larger lesions.

The only baseline parameter with significant influence on RPEL and ELML, and therefore cRORA growth, in this study was the lesion locality. If foveal sparing was present, RPEL and ELML were more important than eyes without foveal sparing. These findings are in concordance with the research performed by Shen et al,[9] stating a lower GA growth rate in lesions with involvement of the foveal center point. Although other studies could detect a significant influence of SDD[31] and lesion focality,[8] this could not be reproduced in our study.

A potential limitation of this study remains the challenges accompanying the application the square root transformation for noncircular lesions.[27] Differing complex growth analysis models have recently been proposed as possible solutions such as the perimeter-adjusted or length-type assessment as they potentially incorporate baseline biomarkers like lesion size and configuration in a more accurate manner into the growth rate assessment.[32,33] Meanwhile, in our analysis, the effect of noncircular lesions could be mitigated by our inclusion of lesion lobularity and focality into the statistical model. In none of our statistical analysis did lesion focality and lobularity reach significance. Further, the missing time point of conversion from iRORA to cRORA in the advanced study cohort, the small sample size, as well as potential segmentation errors must be considered as major limitations of our study. The negative values for the left end point of the 95% CIs can be attributed to minimal segmentation errors by the AI algorithms or biomarker visibility variation on the OCT imaging. Still, these deviations do not impact the validity of our findings but might be a plausible explanation for the large CIs.

Nonetheless, one must consider the challenges of acquiring long-term follow-up data with a starting point at the earliest stages of GA manifestation. The growth from an iRORA toward a cRORA lesion spanning over the complete macular region can take decades. With no approved therapeutic solution in sight at the time, continuous monitoring of cRORA lesions has been of low priority in the last decade.

In conclusion, this study is applying AI-based precision measurements of the subclinical biomarkers relevant to GA disease. We were able to differentially outline the growth rates of cRORA lesions at different progression phases during the natural course of GA secondary to nonneovascular AMD. We observed significantly slower

disease progression in recently developed cRORA lesions measured on SD-OCT. Most importantly, most relevant signs of future disease progression, like photoreceptor degeneration, are already visible during the conversion from iRORA to cRORA. These findings might play a crucial role for the planning of future clinical trials. Individual disease monitoring supported by AI-empowered quantification of neurodegenerative disease activity should be encouraged as early as possible to reconstruct the progression dynamics during the natural course of GA. OCT imaging should be the preferred imaging modality, as it provides a 3-dimensional, in-depth analysis of all retinal layers, particularly at the photoreceptor level, which represents the functional correlate. Important information for disease severity and progression are largely missed with conventional 2-dimensional imaging (e.g., FAF and CFP). More studies on iRORA and early cRORA lesions are needed to determine the ideal point of care and therapeutic target structure for novel progression-slowing therapy.

Footnotes and Disclosures

Originally received: December 23, 2022.
Final revision: April 13, 2023.
Accepted: May 3, 2023.
Available online: May 9, 2023. Manuscript no. ORET-D-22-00779R1.

[1] Vienna Clinical Trial Centre (VTC), Department of Ophthalmology and Optometry, Medical University of Vienna, Vienna, Austria.

[2] Laboratory for Ophthalmic Image Analysis, Department of Ophthalmology and Optometry, Medical University of Vienna, Vienna, Austria.

[3] RetInSight, Vienna, Austria.

Presented at the Association for Research in Vision & Ophthalmology (ARVO) Annual Meeting, Denver, Colorado, May 2022.

Disclosures:

All authors have completed and submitted the ICMJE disclosures form.

The authors made the following disclosures:

U.S.-E.: Research/grant support − Apellis, Genetech, Kodiak, Novartis, RetInSight; Consultant − Apellis, Genentech, Heidelberg Engineering, Kodiak, Novartis, RetInSight, Roche; Patent − RetInSight.

G.S.R.: Research/grant support − RetInSight.

H.B.: Research/grant support − Apellis, Heidelberg Engineering, RetInSight; Honoraria − Apellis, Bayer, Roche.

HUMAN SUBJECTS: Human subjects were included in this study. This study adhered to the tenets of the Declaration of Helsinki and was approved by the Ethics Committee of the Medical University of Vienna in 2011 (EK569.2011). Patients with cRORA secondary to nonneovascular AMD were only included in the study after providing written informed consent.

No animal subjects were used in this study.

Author Contributions:

Conception and design: Coulibaly, Reiter, Bogunovic, Schmidt-Erfurth

Data collection: Coulibaly, Reiter, Fuchs, Lachinov

Analysis and interpretation: Coulibaly, Reiter, Vogl, Leingang, Bogunovic, Schmidt-Erfurth

Obtained funding: The study was performed as part of regular employment duties at the Medical University of Vienna. No additional funding was provided.

Overall responsibility: Schmidt-Erfurth, Reiter, Coulibaly

Abbreviations and Acronyms:
AI = artificial intelligence; **AMD** = age-related macular degeneration; **CAM** = classification of atrophy meetings; **CFP** = color fundus photography; **CI** = confidence interval; **cRORA** = complete retinal pigment epithelial and outer retinal atrophy; **ELM** = external limiting membrane; **ELML** = external limiting membrane loss; **EZ** = ellipsoid zone; **EZL** = ellipsoid zone loss; **FAF** = fundus autofluorescence; **GA** = geographic atrophy; **iRORA** = incomplete retinal pigment epithelial and outer retinal atrophy; **LMM** = linear mixed model; **RPE** = retinal pigment epithelium; **RPEL** = retinal pigment epithelium loss; **SD** = spectral domain; **SDD** = subretinal drusenoid deposit; **VA** = visual acuity.

Keywords:
AI, cRORA, Imaging biomarkers, Non-neovascular AMD, OCT.

Correspondence:
Gregor S. Reiter, MD, Department of Ophthalmology and Optometry, Medical University of Vienna, Währinger Gürtel 18-20, 1090 Vienna, Austria. E-mail: Gregor.reiter@meduniwien.ac.at.

References

1. Wong WL, Su X, Li X, et al. Global prevalence of age-related macular degeneration and disease burden projection for 2020 and 2040: a systematic review and meta-analysis. *Lancet Glob Health*. 2014;2:e106−e116. https://doi.org/10.1016/S2214-109X(13)70145-1.
2. Sarda SP, Heyes A, Bektas M, et al. Humanistic and economic burden of geographic atrophy: a systematic literature review. *Clin Ophthalmol*. 2021;15:4629−4644. https://doi.org/10.2147/OPTH.S338253.
3. Holz FG, Strauss EC, Schmitz-Valckenberg S, van Lookeren Campagne M. Geographic atrophy: clinical features and potential therapeutic approaches. *Ophthalmology*. 2014;121:1079−1091. https://doi.org/10.1016/J.OPHTHA.2013.11.023.
4. Sadda SR, Guymer R, Holz FG, et al. Consensus definition for atrophy associated with age-related macular degeneration on OCT: classification of atrophy report 3. *Ophthalmology*. 2018;125:537−548. https://doi.org/10.1016/J.OPHTHA.2017.09.028.
5. Mahmoudzadeh R, Hinkle JW, Hsu J, Garg SJ. Emerging treatments for geographic atrophy in age-related macular degeneration. *Curr Opin Ophthalmol*. 2021;32:294−300. https://doi.org/10.1097/ICU.0000000000000746.
6. Fleckenstein M, Mitchell P, Freund KB, et al. The progression of geographic atrophy secondary to age-related macular degeneration. *Ophthalmology*. 2018;125:369−390. https://doi.org/10.1016/J.OPHTHA.2017.08.038.
7. Wang J, Ying GS. Growth rate of geographic atrophy secondary to age-related macular degeneration: a meta-analysis of natural history studies and implications for designing future trials. *Ophthalmic Res*. 2021;64:205−215. https://doi.org/10.1159/000510507.

8. Shen LL, Sun M, Grossetta Nardini HK, Del Priore LV. Progression of unifocal versus multifocal geographic atrophy in age-related macular degeneration: a systematic review and meta-analysis. *Ophthalmol Retina*. 2020;4:899−910. https://doi.org/10.1016/J.ORET.2020.03.020.
9. Shen LL, Sun M, Khetpal S, et al. Topographic variation of the growth rate of geographic atrophy in nonexudative age-related macular degeneration: A systematic review and meta-analysis. *Invest Ophthalmol Vis Sci*. 2020;61(1). https://doi.org/10.1167/IOVS.61.1.2.
10. Bui PTA, Reiter GS, Fabianska M, et al. Fundus autofluorescence and optical coherence tomography biomarkers associated with the progression of geographic atrophy secondary to age-related macular degeneration. *Eye (Lond)*. 2022;36:2013−2019. https://doi.org/10.1038/s41433-021-01747-z.
11. Keenan TD, Agrón E, Domalpally A, et al. Progression of geographic atrophy in age-related macular degeneration: AREDS2 report number 16. *Ophthalmology*. 2018;125:1913−1928. https://doi.org/10.1016/J.OPHTHA.2018.05.028.
12. Apellis Announces Top-Line Results from Phase 3 DERBY and OAKS Studies in Geographic Atrophy (GA) and Plans to Submit NDA to FDA in the First Half of 2022. Apellis Pharmaceuticals, Inc. https://investors.apellis.com/news-releases/news-release-details/apellis-announces-top-line-results-phase-3-derby-and-oaks. Accessed May 2, 2022.
13. Lachinov D, Seeböck P, Mai J, et al. Projective skip-connections for segmentation along a subset of dimensions in retinal OCT. *Lecture Notes in Computer Science (including subseries Lecture Notes in Artificial Intelligence and Lecture Notes in Bioinformatics)*. 2021;12901 LNCS:431−441. https://doi.org/10.1007/978-3-030-87193-2_41.
14. Vogl WD, Riedl S, Mai J, et al. Predicting topographic disease progression and treatment response of pegcetacoplan in geographic atrophy quantified by deep learning. *Ophthalmol Retina*. 2023;7:4−13. https://doi.org/10.1016/j.oret.2022.08.003.
15. Riedl S, Vogl WD, Mai J, et al. The effect of pegcetacoplan treatment on photoreceptor maintenance in geographic atrophy monitored by artificial intelligence−based OCT analysis. *Ophthalmol Retina*. 2022;6:1009−1018. https://doi.org/10.1016/j.oret.2022.05.030.
16. Apellis Pharmaceuticals Inc. Apellis protocol no. APL2-304. Phase III, multi-center, randomized, double-masked, sham-controlled study to compare the efficacy and safety of intravitreal APL-2 therapy with sham injections in patients with geographic atrophy (GA) secondary to age-related macular degeneration (AMD) [OAK v3.0], March 19, 2018. Apellis Pharmaceuticals. Identification No. NCT03525613. https://clinicaltrials.gov/ct2/show/study/NCT03525613.
17. Liao DS, Grossi FV, el Mehdi D, et al. Complement C3 inhibitor pegcetacoplan for geographic atrophy secondary to age-related macular degeneration: a randomized phase 2 trial. *Ophthalmology*. 2020;127:186−195. https://doi.org/10.1016/J.OPHTHA.2019.07.011.
18. Apellis Pharmaceuticals Inc. Apellis protocol no. APL2-303. A phase III, multi-center, randomized, double-masked, sham-controlled study to compare the efficacy and safety of intravitreal APL-2 therapy with sham injections in patients with geographic atrophy (GA) secondary to age-related macular degeneration (AMD) [DERBY v3.0], March 19, 2018. Apellis Pharmaceuticals. Identification No. NCT03525600. https://clinicaltrials.gov/ct2/show/study/NCT03525600.
19. Shmueli O, Yehuda R, Szeskin A, et al. Progression of cRORA (complete RPE and outer retinal atrophy) in dry age-related macular degeneration measured using SD-OCT. *Transl Vis Sci Technol*. 2022;11:19. https://doi.org/10.1167/TVST.11.1.19.
20. Mai J, Riedl S, Reiter GS, et al. Comparison of fundus autofluorescence versus optical coherence tomography-based evaluation of the therapeutic response to pegcetacoplan in geographic atrophy. *Am J Ophthalmol*. 2022;244:175−182. https://doi.org/10.1016/J.AJO.2022.06.023.
21. Cleland SC, Konda SM, Danis RP, et al. Quantification of geographic atrophy using spectral domain OCT in age-related macular degeneration. *Ophthalmol Retina*. 2021;5:41−48. https://doi.org/10.1016/J.ORET.2020.07.006.
22. Arslan J, Samarasinghe G, Benke KK, et al. Artificial intelligence algorithms for analysis of geographic atrophy: a review and evaluation. *Transl Vis Sci Technol*. 2020;9:57. https://doi.org/10.1167/TVST.9.2.57.
23. Yehoshua Z, Rosenfeld PJ, Gregori G, et al. Progression of geographic atrophy in age-related macular degeneration imaged with spectral domain optical coherence tomography. *Ophthalmology*. 2011;118:679−686. https://doi.org/10.1016/J.OPHTHA.2010.08.018.
24. Feuer WJ, Yehoshua Z, Gregori G, et al. Square root transformation of geographic atrophy area measurements to eliminate dependence of growth rates on baseline lesion measurements: a reanalysis of age-related eye disease study report no. 26. *JAMA Ophthalmol*. 2013;131:110−111. https://doi.org/10.1001/JAMAOPHTHALMOL.2013.572.
25. Arslan J, Benke KK, Samarasinghe G, Sowmya A, Guymer RH, Baird PN. Model structure uncertainty in the characterization and growth of geographic atrophy. *Transl Vis Sci Technol*. 2021;10:2. https://doi.org/10.1167/TVST.10.6.2.
26. Rudolf M, Vogt SD, Curcio CA, et al. Histologic basis of variations in retinal pigment epithelium autofluorescence in eyes with geographic atrophy. *Ophthalmology*. 2013;120:821−828. https://doi.org/10.1016/j.ophtha.2012.10.007.
27. Monés J, Biarnés M. The rate of progression of geographic atrophy decreases with increasing baseline lesion size even after the square root transformation. *Transl Vis Sci Technol*. 2018;7:40. https://doi.org/10.1167/TVST.7.6.40.
28. Lee KE, Heitkotter H, Carroll J. Challenges associated with ellipsoid zone intensity measurements using optical coherence tomography. *Transl Vis Sci Technol*. 2021;10:27. https://doi.org/10.1167/TVST.10.12.27.
29. Giocanti-Auregan A, Tadayoni R, Fajnkuchen F, Dourmad P, Magazzeni S, Cohen SY. Predictive value of outer retina en face OCT imaging for geographic atrophy progression. *Invest Ophthalmol Vis Sci*. 2015;56:8325−8330. https://doi.org/10.1167/IOVS.14-15480.
30. Pfau M, von der Emde L, de Sisternes L, et al. Progression of photoreceptor degeneration in geographic atrophy secondary to age-related macular degeneration. *JAMA Ophthalmol*. 2020;138:1026−1034. https://doi.org/10.1001/JAMAOPHTHALMOL.2020.2914.
31. Reiter GS, Told R, Schranz M, et al. Subretinal drusenoid deposits and photoreceptor loss detecting global and local progression of geographic atrophy by SD-OCT imaging. *Invest Ophthalmol Vis Sci*. 2020;61:11. https://doi.org/10.1167/IOVS.61.6.11.
32. Shen LL, Sun M, Ahluwalia A, et al. Geographic atrophy growth is strongly related to lesion perimeter: unifying effects of lesion area, number, and circularity on growth. *Ophthalmol Retina*. 2021;5:868−878. https://doi.org/10.1016/J.ORET.2020.12.002.
33. Moult EM, Shi Y, Wang L, et al. Comparing accuracies of length-type geographic atrophy growth rate metrics using atrophy-front growth modeling. *Ophthalmol Sci*. 2022;2:100156. https://doi.org/10.1016/J.XOPS.2022.100156.